J|A|C|S
ARTICLES
Published on Web 03/20/2002

Photoisomerization and Photodissociation of Toluene in Molecular Beam

Chih-Kai Lin, Cheng-Liang Huang, Jyh-Chiang Jiang, A. H. H. Chang,[†] Yuan T. Lee,[‡] S. H. Lin,[‡] and Chi-Kung Ni*

Contribution from the Institute of Atomic and Molecular Science, Academia Sinica, P.O. Box 23-166, Taipei, Taiwan

Received August 29, 2001

Abstract: The photodissociation of isotope-labeled toluene $C_6H_5CD_3$ and $C_6H_5{}^{13}CH_3$ molecules at 6.4 eV under collision-free conditions was studied in separate experiments by multimass ion imaging techniques. In addition to the major dissociation channels, $C_6H_5CD_3 \rightarrow C_6H_5CD_2 + D$ and $C_6H_5CD_3 \rightarrow C_6H_5 + CD_3$, the respective photofragments CD_2H, CDH_2, and CH_3 and their heavy fragment partners C_6H_4D, $C_6H_3D_2$, and $C_6H_2D_3$ were observed from $C_6H_5CD_3$ dissociation. Photofragments $^{13}CH_3$ and CH_3, and their heavy fragment partners C_6H_5 and $^{13}CC_5H_5$, were also observed from $C_6H_5{}^{13}CH_3$ dissociation. Our results show that 25% of the excited toluene isomerizes to a seven-membered ring (cycloheptatriene) and then rearomatizes prior to dissociation. The isomerization pathway competes with *direct* C−C bond and C−H bond dissociation. The significance of this isomerization is that the carbon atoms and hydrogen atoms belonging to the alkyl group are involved in an exchange with those atoms in the aromatic ring during isomerization. The dissociation rate of toluene at 193 nm is measured to be $(1.17 \pm 0.1) \times 10^6$ s^{-1}.

Introduction

Photochemistry processes of benzene and certain alkyl derivatives of benzene have been extensively studied in the past few decades. They are frequently used as examples for both the theoretical and experimental investigation. The most typical monomolecular reactions following the photoexcitation of benzene and its alkyl derivatives are photoisomerization and photodissociation.

For benzene, both the photoisomerization direction and the quantum yield depend on the excitation energy. Fulvene and benzvalene are formed via excitation to the S_1 state, while Dewar benzene is formed from the S_2 state.[1] Benzvalene and Dewar benzene have been obtained only in the condensed phase. The results were interpreted as the formation of benzvalene and Dewar benzene having excess energy that must be rapidly dissipated if they were to survive.[2,3] In addition to the formation of isomers, photodissociation is a major process leading to excited-state benzene in the second singlet state. The major photoproducts of benzene vapor at 184.9 nm were reported to be an isomer of benzene,[4,5] and subsequently identified as fulvene.[6,7] *cis*- and *trans*-1,3-hexadien-5-yne[2,8] and small amounts of methane, ethane, ethylene, hydrogen, and acetylene were also observed.[4,9] The observation of methane, ethane, ethylene, and acetylene indicates dissociation via opening of the aromatic ring. Recently, experiments performed with ue of molecular beams demonstrated that H atom elimination is the major dissociation channel of benzene at 193 nm.[10,11] Two ring-opening dissociation channels, $C_6H_6 \rightarrow CH_3 + C_5H_3$ and $C_6H_6 \rightarrow C_2H_3 + C_4H_3$, were observed. However, they have been found to occur only at higher excitation energy.[11] The dissociation from the S_1 state is very slow, and most of the excited molecules are deactivated through collisions before dissociation occurs.[12]

Toluene is the simplest alkyl derivative of benzene. Photodissociation in the gas phase at 193 nm showed that α-H atom elimination and CH_3 elimination are the major dissociation channels.[13−19] The dissociation rate was found to be 2×10^6

* Addresss correspondence to this author. E-mail: ckni@po.iams.sinica.edu.tw.
[†] Present address: Chemistry Department, National Dong Hwa University, Hualien, Taiwan.
[‡] Also at the Chemistry Department, National Taiwan University, Taipei, Taiwan.

(1) Bryce-Smith, D.; Gilbert, A. *Tetrahedron* **1976**, *32*, 1309−1326.
(2) Ward, H. R.; Wishnok, J. S. *J. Am. Chem. Soc.* **1968**, *90*, 5353−5357.
(3) Wilzbach, K. E.; Ritcher, J. S.; Kaplan, L. *J. Am. Chem. Soc.* **1968**, *89*, 1031−1032.
(4) Foote, J. K.; Mallon, M. H.; Pitts, J. N. *J. Am. Chem. Soc.* **1966**, *88*, 3698−3702.
(5) Shindo, K.; Lipsky, D. *J. Chem. Phys.* **1966**, *45*, 2292−2297.
(6) Ward, H. R.; Wishnok, J. S.; Sherman, P. D., Jr. *J. Am. Chem. Soc.* **1967**, *89*, 162−163.
(7) Kaplan, L.; Wilzbach, K. E. *J. Am. Chem. Soc.* **1967**, *89*, 1030−1031.
(8) Kaplan, L.; Walch, S. P.; Wilzbach, K. E. *J. Am. Chem. Soc.* **1968**, *90*, 5646−5647.
(9) Mellows, F.; Lipsky, S. *J. Phys. Chem.* **1966**, *70*, 4076−4079.
(10) Yokoyama, A.; Zhao, X.; Hintsa, E. J.; Continetti, R. E.; Lee, Y. T. *J. Chem. Phys.* **1990**, *92*, 4222−4233.
(11) Tsai, S.-T.; Huang, C.-L.; Lee, Y. T.; Ni, C.-K. *J. Chem. Phys.* **2001**, *115*, 2449−2455.
(12) Tsai, S.-T.; Lin, C.-K.; Lee, Y. T.; Ni, C.-K. *J. Chem. Phys.* **2000**, *113*, 67−70.
(13) Hippler, H.; Schubert, V.; Troe, J.; Wendelken, H. *J. Chem. Phys. Lett.* **1981**, *84*, 253−256.
(14) Park, J.; Bersohn, R.; Oref, I. *J. Chem. Phys.* **1990**, *93*, 5700−5708.
(15) Fröchtenicht, R. *J. Chem. Phys.* **1994**, *102*, 4850−4859.
(16) Nakashima, N.; Yoshihara, K. *J. Phys. Chem.* **1989**, *93*, 7763−7771.
(17) Luther, K.; Troe, J.; Weitzel, K. L. *J. Phys. Chem.* **1990**, *94*, 6316−6320.
(18) Brand, U.; Hippler, H.; Lindemann, L.; Troe, J. *J. Phys. Chem.* **1990**, *94*, 6305−6316.
(19) Shimada, T.; Ojima, Y.; Nakashima, N.; Izawa, Y.; Yamanaka, C. *J. Phys. Chem.* **1992**, *96*, 6298−6302.

10.1021/ja0120678 CCC: $22.00

s^{-1}, and the proposed dissociation mechanism is *direct* C−H bond and C−C bond rupture, proceeding through the vibrationally excited ground electronic state of toluene, or "hot toluene". Recently, toluene in the S_2 state produced by 200 nm excitation was found to have a fast internal conversion to S_0 and S_1 states with a lifetime of ∼50 fs.[20] The fast internal conversion from initial excited state to lower electronic states and the slow dissociation rate of toluene support the hot molecule reaction mechanism. However, in liquid solutions the dissociation process has proven to be rather inefficient. In liquid solution, the most characteristic monomolecular processes for alkylaromatic compounds is photoisomerization with formation of the derivatives of fulvenes, benzvalenes, Dewar benzene, and prismanes, as well as isomerization with a change in the alkyl substitute's position in the aromatic ring.[21−25] The generally accepted view is that photoisomerization of this kind proceeds by the intermediary formation of isomers such as fulvene, benzvalene, and Dewar benzene with their further rearomatization. It has been suggested that all isomerization processes of benzene and its alkyl derivatives can be described in terms of ring permutation.[26]

Although photodissociation processes of toluene in the S_2 state have been investigated extensively, the photoisomerization of toluene from the S_2 state has until now yet to be reported. In this paper, we report the gas-phase photoisomerization of toluene at 193 nm under collision-free conditions. The isomerization is found to proceed via a six-membered-ring (toluene) to seven-membered-ring (cycloheptatriene) pathway with subsequent rearomatization. This particular isomerization pathway does not belong to the ring permutation, and it has not been reported for any other aromatic molecules. The isomerization reaction competes with the *direct* C−C bond and C−H bond dissociation at the excitation energy of 6.4 eV. The most significant difference between this form of isomerization and that of ring permutation is that the carbon and hydrogen atoms belonging to the alkyl group are involved in the exchange with those atoms in the aromatic ring, whereas in ring permutation isomerization only the hydrogen and carbon atoms belonging to the aromatic ring are involved in the exchange.

Experimental Section

The ion imaging apparatus consisted of a molecular beam, a photolysis laser beam, a VUV probe laser beam, a constant momentum mass spectrometer, and a two-dimensional ion detector. The schematic is shown in Figure 1. The molecular beam, photolysis laser beam, and VUV laser beam were perpendicular to each other. However, the crossing point of the photolysis laser beam with the molecular beam was different from the crossing point of the VUV laser with the molecular beam. The crossing point of the VUV laser beam with the molecular beam was fixed. The crossing point of the photolysis laser beam with the molecular beam was moveable. It was 0−10 cm upstream from the crossing point of the VUV laser with the molecular beam.

Toluene vapor was formed by flowing Ar at a pressure of 300 Torr through a reservoir filled with liquid toluene at 278 K. The toluene−Ar mixture was expanded through a pulsed nozzle and was photodissociated by a 193 nm laser pulse. Due to the recoil velocity and center-of-mass velocity, the fragments expanded to a larger sphere on their flight to the VUV laser beam. Before the VUV laser pulse arrived, the voltage of the extraction plates was set such that any ions produced from the photolysis laser due to multiphoton abosrption were expelled from the entrance of the mass spectrometer. Therefore, no ions resulting from the photolysis laser were detected. After the ejection, the voltages of two extraction plate were set the same, then the VUV laser pulse arrived and ionized the neutral fragments. The distance and time delay between the VUV laser pulse and the photolysis laser pulse was set such that it ensured the VUV laser beam passed through the center of mass of dissociation products, and generated a line of photofragment ions through the center of mass of the dissociation products by photoionization. The length of the segment was proportional to the fragment recoil velocity in the center-of-mass frame multiplied by the delay time between the photolysis laser pulse and the ionization laser pulse. After the ionization, a pulsed electric field was used to extract the ions into a mass spectrometer to separate different masses within the ion segment. While the mass analysis was carried out in the mass spectrometer, the length of the fragment ion segment generated by VUV laser kept expanding according to the fragment recoil velocity. At the exit port of the mass spectrometer, a two-dimensional ion detector was used to detect the ion position and intensity distribution. In this two-dimensional detector, one direction was the recoil velocity axis and the other was the mass axis.

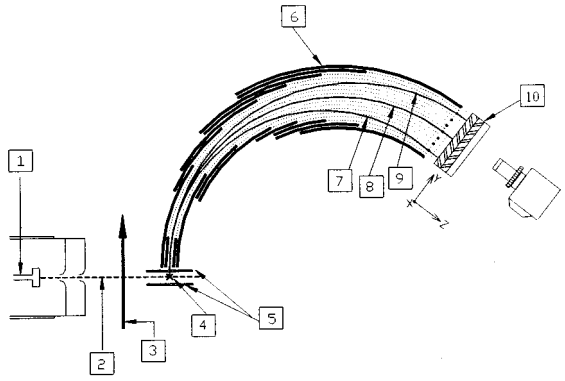

Figure 1. A schematic diagram of the multimass ion imaging detection system: (1) nozzle, (2) molecular beam, (3) photolysis laser beam, (4) VUV laser beam, (5) ion extraction plates, (6) mass spectrometer, (7, 8, 9) simulation trajectories of *m*/*e* 16, 14, and 12, and (10) 2D ion detector.

It is necessary to change the distance between the photolysis laser beam and VUV laser beam to match the delay time between these two laser pulses, according to the velocity of the molecular beam, to ensure the ionization laser will pass through the center of mass of products. This adjustment also changed the length of the fragment ion segment in the image. The relation between the length of ion image and position of the photolysis laser is shown in Figure 2. If the molecules were not dissociated after the absorption of 193 nm photon, these molecules with a lot of internal energy stay within the molecular beam. They fly with the same velocity to the ionization region and are ionized by the VUV laser. The wavelength of the VUV laser in this experiment was set to 118.2 nm; the photon energy of this wavelength is only large enough to ionize toluene molecules. The dissociation of toluene cations would not occur with the energy left after the VUV laser ionization. However, the dissociation could occur following the VUV laser ionization for those hot molecules, which absorb 193 nm photon but did not dissociate. The ion image from the dissociative ionization was very different from the fragment image due to dissociation products of neutral toluene. This image was a 2D projection of the photofragment ion's 3D-recoil velocity distribution. It is very similar to the image from the conventional ion imaging techniques and it is a disklike image. With the VUV laser fixed in position, the size of the disklike image would

(20) Radloff, W.; Freudenberg, Th.; Ritze, H.-H.; Stert, V.; Noack, F.; Hertel, I. V. *Chem. Phys. Lett.* **1996**, *261*, 301−306.
(21) Wilzbach, K. E.; Kaplan, L. *J. Am. Chem. Soc.* **1964**, *86*, 2307−2308.
(22) Burgstahler, A. W.; Chien, P.-L. *J. Am. Chem. Soc.* **1964**, *86*, 2940−2941.
(23) Kaplan, L.; Wilzbach, K. E.; Brown, W. G.; Yang, S. S. *J. Am. Chem. Soc.* **1965**, *87*, 675−676.
(24) Wilzbach, K. E.; Kaplan, L. *J. Am. Chem. Soc.* **1965**, *87*, 4004−4006.
(25) Den Besten, I. E.; Kaplan, L.; Wilzbach, K. E. *J. Am. Chem. Soc.* **1968**, *90*, 5868−5872.
(26) Bryce-Smith, D.; Gilbert, A. In *Rearrangement in Ground and Excited States*; De Mayo, P., Ed.; Academic Press: New York, 1980; Vol. 3.

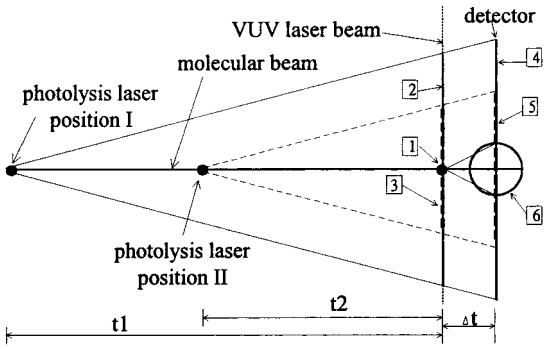

Figure 2. Relationship between the lengths of the image that resulted from different photolysis laser positions as well as the disklike image from the dissociation after ionization. (1) The crossing point of the molecular beam and the VUV laser beam, where the dissociative ionization (reaction 4∼11) occurs. (2 and 3) The lengths of fragment ion segments created by the VUV laser photoionization from two different photolysis laser positions. (4 and 5) The lengths of the fragment ion image on the detector from two different photolysis laser positions. (6) The disklike image from reactions 10. t_1 and t_2 are the two different delay times between the photolysis laser pulse and the VUV laser pulse. Δt is the flight time in the mass spectrometer.

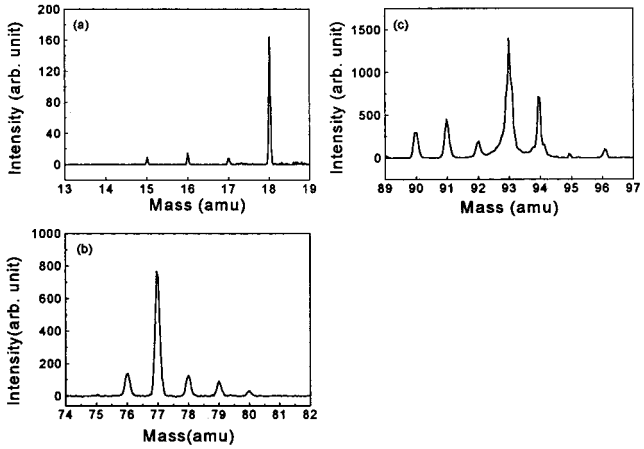

Figure 3. Photofragment time-of-flight mass spectrometry of $C_6H_5CD_3$ in three different mass regions. *M*/*e* 76 (b) and *m*/*e* 90, 91, and 92 (c) fragments result from multiphoton dissociation.

not change with the delay time between two laser pulses, as shown in Figure 2. From the shape of the image and its change with the delay time, the dissociation image of neutral molecules can easily be distinguished from the dissociation image of cation. The disklike image resulting from hot benzene has been observed in a previous study.[11] The experiments have been described in detail elsewhere.[27]

The concentrations of the clusters in the molecular beam were checked by using the VUV laser beam to ionize the species in the beam when the UV photolysis laser beam is not present. A high concentration of dimers was observed in the TOF spectrum when the temperature of the toluene reservoir was higher than 293 K or the Ar pressure was higher than 500 Torr. Dimers were less than 0.1% of monomers under the experimental conditions we used (280 K, 300 Torr).

Results

A. Dissociation of $C_6H_5CD_3$ and $C_6H_5{}^{13}CH_3$. The photofragment TOF mass spectra and images of the fragments are shown in Figures 3 and 4, respectively. In addition to the major fragments, $C_6H_5CD_2$, C_6H_5, and CD_3 from the *direct* dissociation of $C_6H_5CD_3 \rightarrow C_6H_5CD_2 + D$ and $C_6H_5CD_3 \rightarrow C_6H_5 + CD_3$,

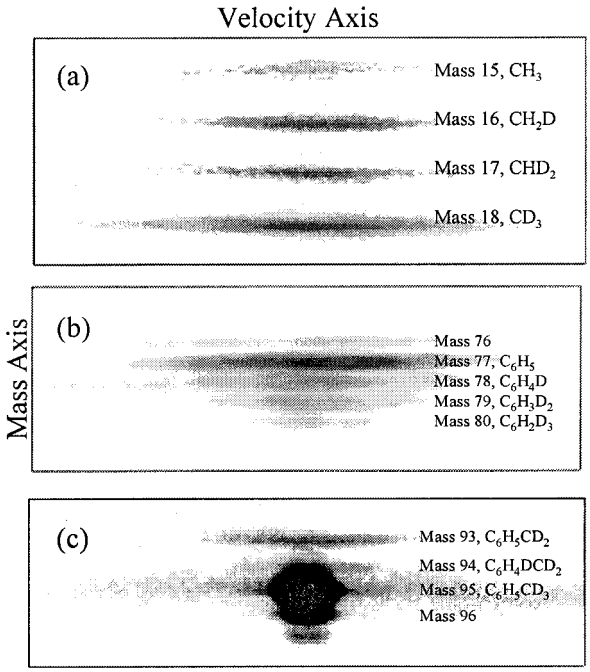

Figure 4. Photofragment ion images of $C_6H_5CD_3$ in three different mass regions. The image of *m*/*e* 76 in part b results from two-photon dissociation. The parent molecule *m*/*e* 95 and *m*/*e* 96 and 97 due to the ^{13}C natural abundance are also shown in image c.

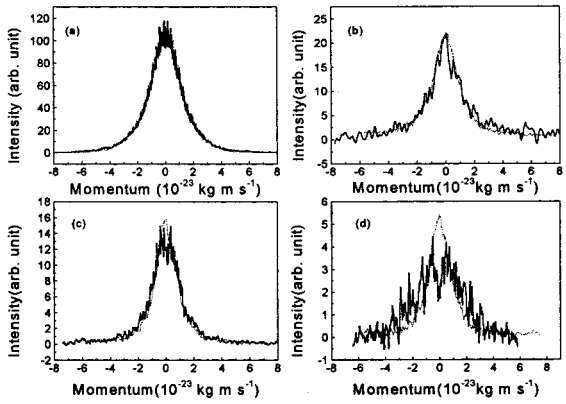

Figure 5. The momentum matches of two fragments in each dissociation channel: (a) *m*/*e* 77 and 18, (b) *m*/*e* 78 and 17, (c) *m*/*e* 79 and 16, and (d) *m*/*e* 80 and 15. The thick lines represent light fragments, and the thin lines represent heavy fragments.

observations of the heavy fragments $C_7H_4D_3$, C_6H_4D, $C_6H_3D_2$, and $C_6H_2D_3$ and the corresponding lighter fragment partners, CD_2H, CDH_2, and CH_3, suggest the existence of the other dissociation channel, i.e., isotope exchange prior to dissociation. Momentum matches of two fragments in each dissociation channel, as shown by Figure 5, further confirm that each fragment pair, C_6H_5 and CD_3, C_6H_4D and CD_2H, $C_6H_3D_2$ and CDH_2, and $C_6H_2D_3$ and CH_3, is from the dissociation of C_6H_5-CD_3. These momentum matches also exclude the contribution from three-body dissociation, like the dissociation of clusters, or the contribution from cation dissociation. Measurements of the fragment intensities as a function of photolysis laser power show that all of these dissociation channels result from one-photon dissociation, as illustrated in Figure 6. The results from one-photon dissociation were also confirmed by the photofragment translational energy distribution. Figure 7 shows that the fragment maximum translational energy does not exceed the

(27) Tsai, S.-T.; Lin, C.-K.; Lee, Y. T.; Ni, C.-K. *Rev. Sci. Instrum.* **2001**, *72*, 1963−1969.

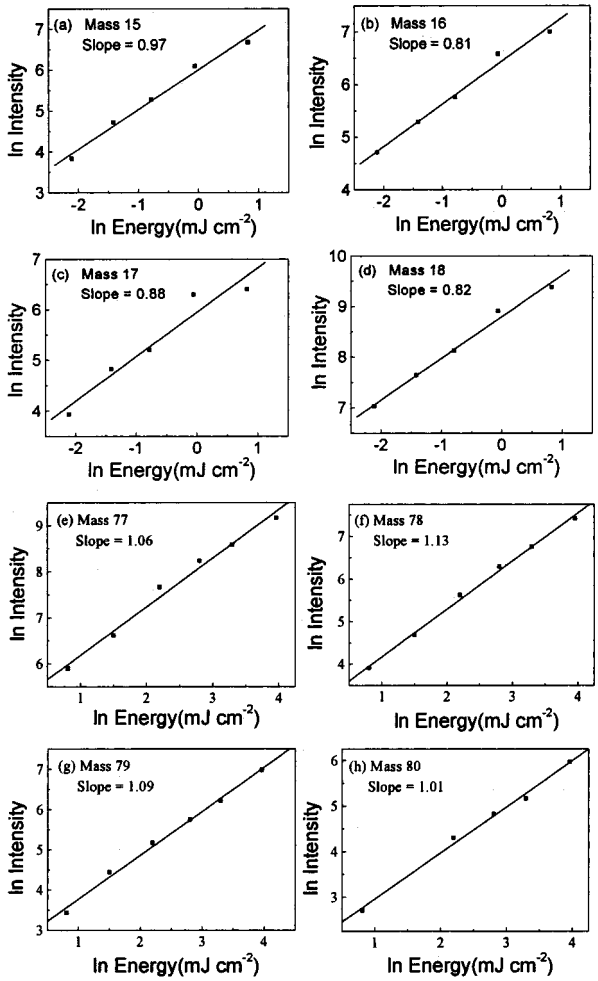

Figure 6. Photofragment intensities as a function of photolysis laser power. It shows all the fragments are result from one photon dissociation.

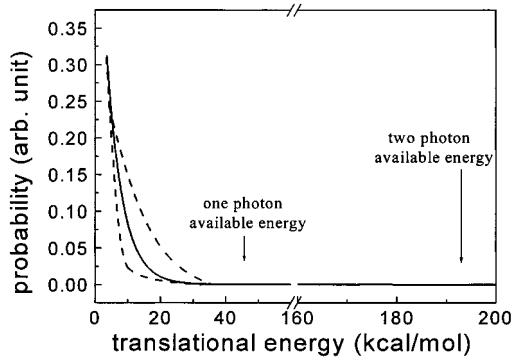

Figure 7. Photofragment translational energy distribution from reactions 3b and 8b. The translational energy distributions are the same for reactions 3b and 8b within experimental uncertainty. The solid line represents the experimental measurement, and the dotted lines represent upper and lower limits due to experimental uncertainty.

available energy (= photon energy − bond energy) from one 193 nm photon. The product buildup times of the respective photofragments C_6H_5, C_6H_4D, $C_6H_3D_2$, $C_6H_2D_3$, $C_7H_5D_2$, and $C_7H_4D_3$, originating from $C_6H_5CD_3$, are shown in Figure 8. The product buildup times of production of C_6H_5 are very close to the measurements in previous study.[14,28,29]

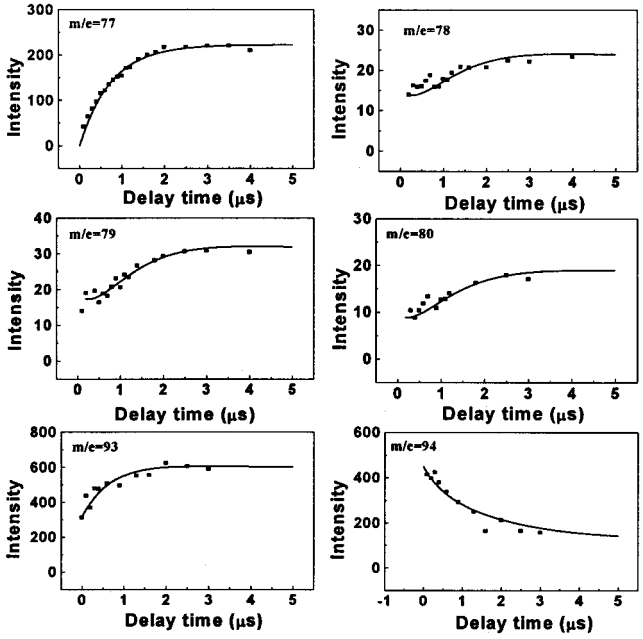

Figure 8. The product buildup times. The solid line is the simulation from reactions 1−10. The nonzero intensity at $t = 0$ and the intensity decay of *m*/*e* 94 are due to the dissociative ionization (reaction 10).

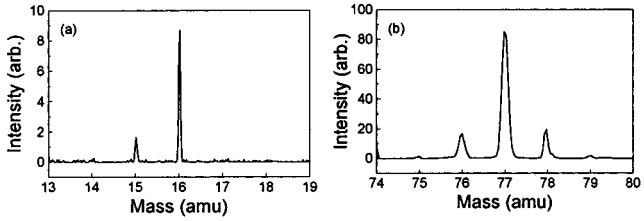

Figure 9. The photofragment TOF mass spectrometry from the dissociation of $C_6H_5{}^{13}CH_3$ in two different mass regions. The *m*/*e* 76 fragment results from multiphoton dissociation.

The photofragment TOF mass spectra resulting from the dissociation of $C_6H_5{}^{13}CH_3$ are shown in Figure 9. In addition to the major dissociation channel, $C_6H_5{}^{13}CD_3 \rightarrow C_6H_5 + {}^{13}CH_3$, the observation of $^{13}CC_5H_5$ and CH_3 indicates that the methyl carbon atom is involved in the exchange with aromatic carbon atoms prior to dissociation. Table 1 gives the relative ion intensity of the fragments.

B. Impurity Effects. To ensure that the extraordinary high ratios of the "unexpected" fragments, C_6H_4D, $C_6H_3D_2$, $C_6H_2D_3$, CD_2H, CDH_2, and CH_3, are not the result of sample impurities, mass spectrometry and NMR spectra are used to check the impurity levels.

$C_6H_5CD_3$ (99% D atom) was purchased from Cambridge Isotope Inc. Figure 10a shows the mass spectrum of $C_6H_5CD_3$ obtained by VUV photoionization. Three peaks, *m*/*e* 94, 95, and 96, were observed, corresponding to the impurity of $C_7H_6D_2$, the parent molecule $C_7H_5D_3$, and $^{13}CC_6H_5D_3$ as due to the ^{13}C natural abundance, respectively. The VUV photon energy is set at 10.5 eV. The VUV photon energy is low enough such that only ionization processes occur, the dissociation of toluene cations would not occur with the energy left after the VUV photoionization. On the other hand, this VUV photon energy is much higher than the toluene ionization threshold (8.8 eV), so

(28) Kajii, Y.; Obi, K.; Tanaka, I.; Ikeda, N.; Nakashima, N.; Yoshihara, K. *J. Chem. Phys.* **1987**, *86*, 6115−6118.

(29) Ikeda, N.; Nakashima, N.; Yoshihara, K. *J. Chem. Phys.* **1985**, *82*, 5285−5286.

Table 1. The Experimental and Statistical Fragment Intensity Ratios between *m*/*e* 15, 16, 17, and 18 and between *m*/*e* 77, 78, 79, and 80

	mass (*m*/*e*)											
	15	16	17	18	77	78		79			80	
formula	CH_3	CH_2D	CH_2D	CD_3	C_6H_5	C_6DH_4	$^{13}CC_5H_5$	$C_6D_2H_3$	$^{13}CC_5DH_4$	$^{13}C_2C_4DH_4$	C_6D_3H	$^{13}CC_5DH_4$
exptl[a]	5.6	9.5	6.2	100	100	7.9	6.6	9.1	0.5	0.4	3.3	0.6
statistical[b]	10	30	15	1	1	15		30			10	

[a] The experimental results of *m*/*e* 18 and 77 contain direct dissociation and indirect dissociation. [b] The statistical results of *m*/*e* 18 and 77 contain only the indirect dissociation.

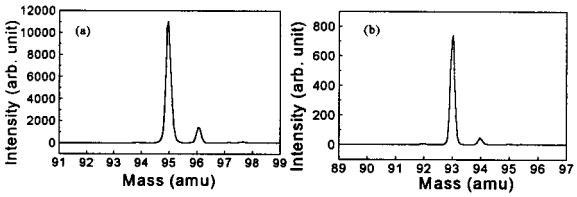

Figure 10. VUV photoionization/TOF mass spectrum of (a) $C_6H_5CD_3$ and (b) $C_6H_5{}^{13}CH_3$. The VUV photon energy is 10.5 eV.

that large differences of ionization cross sections due to isotopic effects would not be expected to occur. As a consequence, the ion intensity of each mass obtained from VUV photoionization is directly proportional to the relative concentration of each mass. The TOF mass spectrum shows that the relative intensities of $C_7H_6D_2$, $C_7H_5D_3$, and $^{13}CC_6H_5D_3$ are 0.6:100:8.1. These ratios indicate that the ratio of fragments CHD_2:CD_3 resulting from photodissociation should be 0.6:100 if isotope scrambling does not occur during the dissociation process. Our experimental results illustrate that the respective fragment ratios for CH_3:CH_2D:CHD_2:CD_3 are 5.6 ± 0.9:9.5 ± 0.2:6.2 ± 1.1:100. The relative amount of CHD_2 obtained in our experiment is 10 times larger than the amount due to impurity. Additionally, the relative amounts of CH_3 and CH_2D obtained in our experiment are at least 100 times larger than the amount due to impurity. Similar ratios are obtained for the heavy fragments C_6H_4D, $C_6H_3D_2$, and $C_6H_2D_3$, as shown in Table 1.

The mass spectra of $C_6H_5{}^{13}CH_3$ (Cambridge Isotope Inc 98%) obtained using VUV photoionization at 10.5 eV is shown in Figure 10b. Three peaks, *m*/*e* 92, 93, and 94, were observed, corresponding to the impurity of C_7H_8, the parent molecule $C_6H_5{}^{13}CH_3$, and $^{13}CC_5H_5{}^{13}CH_3$ as a consequence of ^{13}C natural abundance. The spectrum reveals that the relative ratios of C_7H_8, $C_6H_5{}^{13}CH_3$, and $^{13}CC_5H_5{}^{13}CH_3$ are 1.0:100:6.4. The experimental ratio of fragments CH_3:$^{13}CH_3$ is 21:100, which is 21 times larger than the ratio of impurity if isotope scrambling does **not** occur in the photodissociation process.

The impurity level in the sample is also measured by ^1H NMR spectroscopy. The NMR spectrum of $C_6H_5CD_3$ shows that the amount of toluene with H atoms in the methyl group is 0.5%. This value is very close to the 0.6% impurity level measured by mass spectrometry. The result also suggests that most of the impurity having *m*/*e* 94 has the structure $C_6H_5CD_2H$. The NMR spectrum of $C_6H_5{}^{13}CH_3$ also shows that there is only 1.2% impurity of non-^{13}C-substituted toluene, $C_6H_5{}^{12}CH_3$. These results are consistent with the result from mass spectra, and the amount of impurity is 22 times smaller than the fragment for CH_3 that we observed. Measurements from both mass spectra and NMR indicate that impurity levels are sufficiently small and may be neglected in our results.

Discussions

A. Isomerization Mechanism. The gas-phase photoisomerization of 1,3,5-cycloheptatriene (CHT) to toluene and the subsequent dissociation of toluene to a benzyl radical and a hydrogen atom were first proposed in 1962.[30,31] The quantum yield of toluene was found to increase with decreasing pressure, with the extrapolated value to zero pressure being given by unity. It was suggested that isomerization to toluene occurs not from electronically excited molecules of cycloheptatriene but from a vibrationally excited ground state molecule formed via internal conversion of the electronic energy. The thermal isomerization rate in shock waves and the photoisomerization rate between 238 and 289 nm of CHT, methyl-CHT, and ethyl-CHT have been accurately measured.[32−34] Additionally, it was found that the H atom migration within the seven-membered ring is much faster than the isomerization.[33] The isomerization rate of CHT to toluene using 248.4 nm photons was found to be 1.8×10^8 s^{-1}, and the subsequent dissociation of toluene was found to be 3×10^6 s^{-1},[13,35] which is very close to the dissociation rate of toluene at the same energy.[14,28,29] The photofragments C_6H_5 and $C_6H_5CH_2$ have been observed in the photodissociation of CHT at both 248 and 266 nm in molecular beam experiments.[36,37] The same photofragments are also observed in the photodissociation of toluene at 193 nm.[15−18] These studies support the mechanism proposed in a previous study, i.e., CHT isomerizes to toluene prior to dissociation. The investigation by Bersohn[14] of CHT-*1,1-d*$_2$ photodissociation at 248.4 nm showed that the isotopic scrambling of D and H atoms is complete prior to the isomerization from CHT to toluene.

Although the seven-membered-ring (CHT) to six-membered-ring (toluene) isomerization has been observed experimentally, the reverse reaction has yet to be reported. This is likely because the reverse reaction has a higher activation energy, resulting in a smaller isomerization rate. The isomerization channel also has to compete with fast dissociation channels, and therefore isomerization would not be easily observed. As a result, all dissociation mechanisms of toluene after the 193 nm excitation have been interpreted as direct C−H bond or C−C bond cleavages after internal conversion.

Our observation of small amount of CD_2H, CDH_2, and CH_3 and their heavy fragment partners, C_6H_4D, $C_6H_3D_2$, and $C_6H_2D_3$, from the dissociation of $C_6H_5CD_3$ clearly indicates that direct C−H bond and C−C bond cleavage is not the only dissociation

(30) Srinivasan, R. *J. Am. Chem. Soc.* **1962**, *84*, 3432−3436.
(31) Thrush, B. A.; Zwolenik, J. J. *Bull. Soc. Chim. Belg.* **1962**, *71*, 642−650.
(32) Astholz, D. C.; Troe, J.; Wieters, W. *J. Chem. Phys.* **1979**, *70*, 5107−5116.
(33) Troe, J.; Wieters, W. *J. Chem. Phys.* **1979**, *71*, 3931−3941.
(34) Hippler, H.; Luther, K.; Troe, J.; Wendelken, H. *J. Chem. Phys.* **1983**, *79*, 239−246.
(35) Tsukiyama, K.; Bersohn, R. *J. Chem. Phys.* **1987**, *86*, 745−749.
(36) Krajnovich, D. J. Ph.D. Thesis, University of California, Berkeley, 1983.
(37) Brudzynski, R. J. Ph.D. Thesis, University of California, Berkeley, 1983.

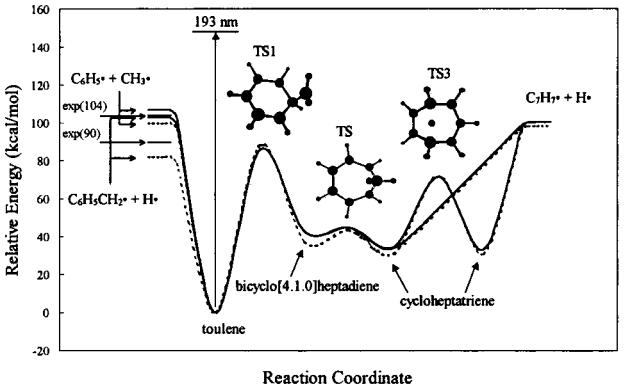

Figure 11. Energy diagram for isomerization and dissociation reactions of toluene. The energies shown are computed at B3LYP/aug-cc-pVTZ (solid line) and CCSD/6-311+G* (dash line) at the geometry optimized by B3LYP/6-31+G*.

mechanism. Another dissociation mechanism must exist, which allows for the exchange of D atoms in the methyl group with H atoms in the aromatic ring prior to dissociation. The respective ratios between CD_2H, CDH_2, and CH_3, and those ratios between C_6H_4D, $C_6H_3D_2$, and $C_6H_2D_3$ from experiment are very close to the statistical values, as given in Table 1. This suggests that a small fraction of parent molecules enter the other dissociation channel. The isotopic scrambling of D and H atoms between the methyl group and the aromatic group in this channel is almost complete before dissociation occurs. The small amount of CH_3 resulting from $C_6H_5{}^{13}CH_3$ dissociation indicates that not only are hydrogen atoms involved in the scrambling, but also that carbon atoms in both the methyl group and the aromatic group are involved in the exchange. The results cannot be explained by the existing isomerization mechanisms for aromatic molecules, i.e., ring permutation, because the ring permutation involves only hydrogen and carbon atom exchange within the aromatic group.

A reasonable isomerization mechanism that explains the experimental results is the isomerization from a six-membered ring (toluene) to a seven-membered ring (cycloheptatriene). After isomerization to a seven-membered ring, isotopic scrambling of the H/D and carbon atoms occurs through H or D atom migration around the seven-membered ring. In the end, the rearomatization of cycloheptatriene to toluene and the subsequent dissociation through C−C bond cleavage results in the formation of fragments CD_2H, CDH_2, and CH_3, and their heavy fragment partners, C_6H_4D, $C_6H_3D_2$, and $C_6H_2D_3$. Hydrogen or D atom elimination can occur from cycloheptatriene, or occur after the rearomatization of cycloheptatriene to toluene. The same mechanism can be used to explain the formation of the respective photofragments CH_3, $^{13}CH_3$, C_6H_5, $C_5{}^{13}CH_5$ from the dissociation of $C_6H_5{}^{13}CH_3$.

This particular isomerization pathway is supported by ab initio calculations. The energies of isomers and various transition states along the isomerization pathway from ab initio calculation are shown in Figure 11. The dissociation of toluene has barrier heights of 89.7 kcal/mol for C−H bond cleavage, and 103.8 kcal/mol for C−C bond cleavage. The six-membered-ring to seven-membered-ring isomerization has a barrier height of 84.9 kcal/mol. Since the barrier heights are all very close in energy, direct C−C bond and C−H bond dissociation competes with isomerization. Most of the toluene molecules dissociate directly through C−C and C−H bond cleavages after the internal conversion. However, a small fraction of toluene molecules isomerize to CHT. The migration of H or D atoms in CHT due to the low barrier height results in isotopic scrambling of D/H atoms and carbon atoms in CHT. Fast H-atom and D-atom scrambling in CHT is consistent with the complete isotopic scrambling of CHT excited by 248 nm photons in the previous study.[14] Table 1 displays the statistical ratio of different fragments if the isotopic scrambling of D/H atoms in cycloheptatriene is complete. The comparison between the experimental result and the statistical ratio illustrates that the isotopic scrambling of D/H atoms in cycloheptatriene is nearly complete.

B. Kinetic Model. The results of the experiments can be described by using the following reactions.

$$C_6H_5CD_3 + h\nu_{193nm} \rightarrow C_6H_5CD_3^* \text{ (excitation)} \quad (1)$$

$$C_6H_5CD_3^* \rightarrow C_6H_5CD_3^{\ddagger} \text{ (internal conversion)} \quad (2)$$

$$C_6H_5CD_3^{\ddagger} \rightarrow C_6H_5CD_2 + D \text{ (direct dissociation after internal conversion)} \quad (3a)$$

$$C_6H_5CD_3^{\ddagger} \rightarrow C_6H_5 + CD_3 \text{ (direct dissociation after internal conversion)} \quad (3b)$$

$$C_6H_5CD_3^{\ddagger} \rightarrow c\text{-}C_7H_5D_3^{\ddagger} \text{ (isomerization)} \quad (4)$$

$$c\text{-}C_7H_5D_3^{\ddagger} \rightarrow c\text{-}C_7H_5D_3^{\ddagger} \text{ (isotopic scrambling)} \quad (5)$$

$$c\text{-}C_7H_5D_3^{\ddagger} \rightarrow c\text{-}C_7H_{5-x}D_{2+x} + H \text{ (or D) } (x = 0, 1) \text{ (7-membered-ring dissociation)} \quad (6)$$

$$c\text{-}C_7H_5D_3^{\ddagger} \rightarrow C_6H_{5-x}D_xCH_xD_{3-x}{}^{\ddagger} \ (x = 0, 1, 2, 3) \text{ (rearomatization)} \quad (7)$$

$$C_6H_{5-x}D_xCH_xD_{3-x}{}^{\ddagger} \rightarrow C_6H_{5-x}D_xCH_{x-1}D_{3-x} + H \ (x = 1, 2, 3) \text{ or } C_6H_{5-x}D_xCH_xD_{3-x-1} \ (x = 0, 1, 2, 3) \text{ (dissociation after rearomatization)} \quad (8a)$$

$$C_6H_{5-x}D_xCH_xD_{3-x}{}^{\ddagger} \rightarrow C_6H_{5-x}D_x + CH_xD_{3-x} \ (x = 0, 1, 2, 3) \text{ (dissociation after rearomatization)} \quad (8b)$$

All of the dissociation products from reaction 3, 6, and 8 were ionized by VUV laser and detected by ion image detector. They can be represented by the following reaction

$$P + h\nu_{VUV} \rightarrow P^+ \ (P = C_6H_{5-x}D_x, CH_xD_{3-x}, C_7H_5D_2, C_7H_4D_3) \quad (9)$$

However, at very short delay time, some of the hot toluene which has not dissociated into fragments could absorb the VUV photon and result in dissociative ionization.

$$C_6H_5CD_3^{\ddagger} + h\nu_{VUV} \rightarrow C_6H_{5-x}D_xCH_{x-1}D_{3-x}{}^+ + H \ (x = 1, 2, 3) \quad (10a)$$

$$\text{or } C_6H_{5-x}D_xCH_xD_{3-x-1}{}^+ + D \ (x = 0, 1, 2) \quad (10b)$$

$$C_6H_5CD_3^{\ddagger} + h\nu_{VUV} \rightarrow C_6H_{5-x}D_x^{+} + CH_xD_{3-x} \quad (x = 0, 1, 2, 3) \quad (10c)$$

The ion from these dissociative ionization channels produces the background at short delay time. The nonzero intensity at $t = 0$ and the intensity decay of m/e 94 in Figure 8 are due to this background. However, at long delay time, most of the hot toluene dissociates into fragments, and this background decays to zero. The dissociation lifetime, $1/k_3$ ($=1/(k_{3a} + k_{3b})$) = 850 ns at 193 nm, is very short compared to the delay time between pump and probe laser pulses ($\sim$30 μs) in imaging experiments, therefore, most of the hot toluene molecules dissociate into fragments and only the line-shape images were observed. The photodissociation and photoisomerization of $C_6H_5{}^{13}CH_3$ can also be described by the similar reactions.

Reactions 1−10 are used to simulate the apparent rate and the relative intensity of the fragments. We neglect the reactions 1 and 2 since they are very fast compared to the other reactions. In addition, due to the low S/N ratio in the product apparent rates and the large number of isotopic isomers of cycloheptatriene and toluene, it is impossible to simulate the result including all the possible isotopic effects. One of the isotopic effects, which is the effect on the H and D atom elimination channels (reaction 8a), has been measured by Bersohn.[14] They found that the H atom fragment intensity is 3.6 times higher than the D atom fragment intensity from photodissociation of $C_6H_5CH_2D$ and concluded that the ratio of H:D atom elimination due to the isotopic effect is 1.8. However, since they did not consider the isotope exchange due to the six-membered-ring to seven-membered-ring isomerization, the ratio they measured is the upper limit.

In the simulation, we neglect all the isotopic effects except those on the H and D atom elimination channels (reaction 3a and 8a), the isotopic effect of which is expected to be large. We assume that $k_4 = k_{-7}$, $k_7 = k_{-4}$, $k_5 = k_{-5}$, and $k_{3b} = k_{8b}$. The simulation result shows that k_3 ($=k_{3a} + k_{3b}$) is very sensitive to the apparent rate of fragment m/e 77. This is because most of the fragments of m/e 77 come from reaction 3. However, the value of k_5 is not sensitive with respect to the final results as long as its value is 50 times larger than that for k_7. This is because the result will not be changed by the increase of the scrambling rate after the isotopic scrambling is complete. On the other hand, the best value of k_7 is $(1 \pm 0.3) \times 10^8$ s^{-1} in order to fit the apparent rate of fragments m/e 78, 79, and 80.

For the H or D atom elimination channel, they could result from the seven-membered-ring dissociation (reaction 6) or from the six-membered-ring dissociation (reactions 3a and 8a). However, our result is not sensitive to k_6 when it is smaller than 1×10^7 s^{-1}. As a result, the upper limit of k_6 is 1×10^7 s^{-1}. Although the upper limit of the dissociation rate from the seven-membered ring is larger than the dissociation rate from the six-membered ring, the dissociation from seven-membered ring must compete with the rearomatic process. Since the rearomatic rate is at least 10 times larger than the upper limit of the seven-membered-ring dissociation rate, it is not likely that the dissociation from seven-membered ring is important. The simulation results are shown in Figure 8. From the simulation, we obtain k_3 ($=k_{3a} + k_{3b}$) = $(1.17 \pm 0.08) \times 10^6$ s^{-1}, $k_4 = (3.4 \pm 0.3) \times 10^5$ s^{-1}, $k_5 > 5 \times 10^8$ s^{-1}, $k_6 < 1 \times 10^7$ s^{-1}, and the ratio of H atom and D atom elimination from methyl group of toluene of 1.6 ± 0.2. Values for k_3, k_5, and k_7 are very close to those from previous studies of toluene[14,28,29] and CHT.[13,14,33] The $k_4/(k_3 + k_4)$ ratio shows that about 25 $\pm$ 4% of hot toluene molecules isomerize to cycloheptatriene, followed by H and D atom exchange in cycloheptatriene, and subsequent rearomatization to toluene prior to dissociation.

The dissociation of toluene and the isomerization between cycloheptatriene and toluene in the ground electronic state are standard unimolecular reactions. They can be characterized by RRKM calculation. We used the potential energy surface obtained from ab initio calculation (B3LYP/6-31+G*) and performed the variational RRKM calculation for various reaction rates. The results of RRKM calculation show that the isomerization rate form toluene to bicycloheptadiene is 1.5×10^4 s^{-1}, and the reverse reaction has the rate of 9×10^7 s^{-1}. The subsequent isomerization from bicycloheptadiene to cycloheptatriene is 3×10^{12} s^{-1}, and the reverse reaction is 5×10^{11} s^{-1}. The hydrogen migration in the cycloheptatriene has a rate of 1×10^{12} s^{-1}. The H atom elimination from cycloheptatriene and toluene has the rates of 1×10^1 and 0.43 s^{-1}, respectively. The result shows that the isomerization rate is determined by the step from toluene to bicycloheptadiene and the subsequent isomerization to CHT is fast enough to be neglected. Additionally, the hydrogen migration in the cycloheptatriene is so fast that the isotope scrambling is complete prior to rearomatization and dissociation. Comparison with the experimental result shows that the calculated rearomatization rate agrees with our experimental value and previous studies very well,[13,33,35] and the calculated isomerization rate is close to the experimental value. On the other hand, the discrepancy is significant for reactions 3 and 5. The calculated H atom migration rate within the seven-membered ring is overestimated, and the H atom elimination rate from toluene is underestimated. In fact, the potential energy curve used in the variational RRKM calculation for H atom elimination has a dissociation threshold 10 kcal/mol higher than the experimental measurement. Even if the experimental value of the dissociation threshold is used in the RRKM calculation, it shows that the H atom elimination has a rate of 3×10^3 s^{-1}, which is still small compared to the experimental value. As a result, the percentage of hot toluene molecules that isomerize to cycloheptatriene prior to dissociation is overestimated by calculation. Although some of the calculated values are significantly different from the experimental values, the calculated reaction rates are in agreement with the experimental results in the phenomena such that H atom migration in CHT is faster than the rearomatization and the dissociation rate in CHT is slow compared to rearomatization.

It is interesting to note that these reaction rates were obtained at a fixed internal energy (one 193 nm photon energy). These reaction rates vary rapidly with the change of internal energy, therefore the dissociation branching ratios and the ratio between direct dissociation and isomerization are expected to be different at the different energy.

Conclusions

We have observed the six-membered-ring to seven-membered-ring isomerization of toluene at an excitation energy of 6.4 eV. About 25% of "hot" toluene molecules isomerize to the seven-membered ring (cycloheptatriene) and subsequently rearomatization prior to dissociation. Although the percentage is small,

it is clearly not negligible. This is the first time that this kind of isomerization was experimentally observed in aromatic molecules. The most significant difference of this particular isomerization channel from that of other aromatic isomerization pathways is that alkyl carbon and hydrogen atoms are involved in the exchange with those atoms in the aromatic ring during this isomerization process. This is unlike that found in ring permutation isomerization, in which only the hydrogen and carbon atoms of the aromatic ring are involved in the exchange.

Acknowledgment. This work was partially supported by the National Science Council under contract NSC 89-2113-M-001-083 and the China Petroleum Corporation, Taiwan.

JA0120678